

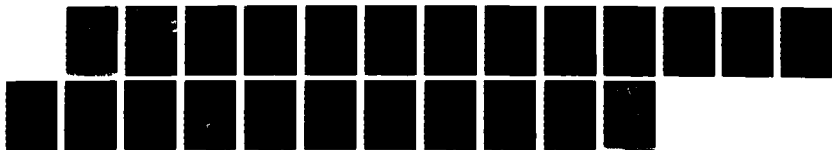
AD-A184 632

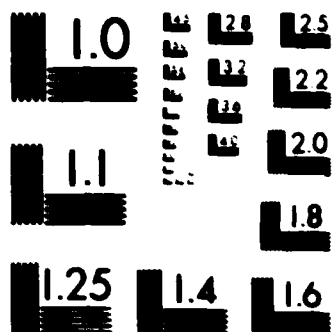
TON-MATRIX COUPLING IN POLYMER ELECTROLYTES FROM
RELAXATION TIME STUDIES ALCOHOL OBTAINED FROM THEN(U)
PURDUE UNIV LAFAYETTE IN DEPT OF CHEMISTRY 84 AUG 87
TR-13 F/G 7/4

1/1

UNCLASSIFIED

NL





MICROCOPY RESOLUTION TEST CHART
NATIONAL BUREAU OF STANDARDS-1963-A

DTIC FILE COPY

62

AD-A184 632

REPORT DOCUMENTATION PAGE

1. UNCLASSIFIED		1b. RESTRICTIVE MARKINGS	
2a. SECURITY CLASSIFICATION AUTHORITY		3. DISTRIBUTION AVAILABILITY OF REPORT Approved for public release and sale; its distribution is unlimited.	
2b. DECLASSIFICATION/DOWNGRADING SCHEDULE		5. MONITORING ORGANIZATION REPORT NUMBER(S)	
4. PERFORMING ORGANIZATION REPORT NUMBER(S) Technical Report No. 13		7a. NAME OF MONITORING ORGANIZATION Division of Sponsored Programs Purdue Research Foundation	
6a. NAME OF PERFORMING ORGANIZATION Purdue University Department of Chemistry	6b. OFFICE SYMBOL (If applicable)	7b. ADDRESS (City, State, and ZIP Code) Purdue University West Lafayette, IN 47907	
8a. NAME OF FUNDING SPONSORING ORGANIZATION Office of Naval Research	8b. OFFICE SYMBOL (If applicable)	9. PROCUREMENT INSTRUMENT IDENTIFICATION NUMBER	
8c. ADDRESS (City, State, and ZIP Code) 800 N. Quincy Street Arlington, VA 22217		10. SOURCE OF FUNDING NUMBERS	
		PROGRAM ELEMENT NO	PROJECT NO
		TASK NO	WORK UNIT ACCESSION NO
11. TITLE (Include Security Classification) Ion-Matrix Coupling in Polymer Electrolytes from Relaxation Time Studies			
12. PERSONAL AUTHOR(S) L.M. Torelli and C.A. Angell			
13a. TYPE OF REPORT Technical	13b. TIME COVERED FROM 2/1/87 TO 8/4/87	14. DATE OF REPORT (Year, Month, Day) 1987, August, 4	15. PAGE COUNT
6. SUPPLEMENTARY NOTES Polymer Journal			
17. COSAT CODES		18. SUBJECT TERMS (Continue on reverse if necessary and identify by block number)	
FIELD	GROUP	conductivity, polymer electrolyte, block polymer, microphase separation	
19. ABSTRACT (Continue on reverse if necessary and identify by block number) We review the effects of temperature on conductance and viscosity in the liquid state of vitreous ionic conductors and show how differences may be best understood by comparison of relaxation times for electrical and mechanical stressers acting on liquid or glassy states of the material. This leads to the definition of a conductivity/viscosity mode decoupling index, useful as a figure of merit for the solid electrolyte. In applying the same approach to polymer electrolyte systems a problem is encountered due to the molecular weight dependence of the viscosity. This is resolved by deriving a "monomer" shear relaxation time for the polymer electrolyte solution and showing that this quantity corresponds closely with the "local" mechanical relaxation time obtained from light scattering studies (which is a molecular weight independent quantity for pure polymers). Comparison of the electrical relaxation times of the polymer solution with the "local" (or "matrix") relaxation times then shows that the relationship found for superionic glassforming systems is inverted in the case of polymer electrolytes. The latter have fractional decoupling indexes which may be interpreted in terms of serial (continued on back)			
20. DISTRIBUTION AVAILABILITY OF ABSTRACT <input type="checkbox"/> UNCLASSIFIED/LIMITED <input checked="" type="checkbox"/> SAME AS RPT <input type="checkbox"/> DTIC USERS		21. ABSTRACT SECURITY CLASSIFICATION Unclassified	
22a. NAME OF RESPONSIBLE INDIVIDUAL		22b. TELEPHONE (Include Area Code)	22c. OFFICE SYMBOL

19. (continued)

coupling phenomena; i.e. ions must first decouple from their partner ions (in ion pairs), or from their intramolecular solvation states, before they can contribute to conductivity relaxation which is itself coupled to the local polymer matrix relaxation. An extreme case is illustrated using the weak electrolyte, lithium acetate, for which the decoupling index is $\sim 6 \times 10^{-5}$.

OFFICE OF NAVAL RESEARCH

Contract No. N0014-84-K0289

TECHNICAL REPORT, AUGUST 1987

ION-MATRIX COUPLING IN POLYMER ELECTROLYTES
FROM RELAXATION TIME STUDIES

L.M. Torell and C.A. Angell

Prepared for publication
in the
Polymer Journal

Purdue University
Department of Chemistry
West Lafayette, IN 47907

August 1987

Prepared for

Office of Naval Research
800 N. Quincy Street
Arlington, VA 22217

Division of Sponsored Programs
Purdue Research Foundation
Purdue University
West Lafayette, IN 47907



Accession For	
NTIS CRA&I	<input checked="" type="checkbox"/>
DTIC TAB	<input type="checkbox"/>
Unannounced	<input type="checkbox"/>
Justification	
By	
Distribution/	
Availability Codes	
Dist	Acad and/or Special
A-1	

87 9 10 198

ION-MATRIX COUPLING IN POLYMER ELECTROLYTES FROM RELAXATION TIME STUDIES

L.M. Torell
Department of Physics
Chalmers University of Technology
Goteborg, S-41296, SWEDEN

and

C.A. Angell
Department of Chemistry
Purdue University
West Lafayette, IN 47906, USA

ABSTRACT

We review the effects of temperature on conductance and viscosity in the liquid state of vitreous ionic conductors and show how differences may be best understood by comparison of *relaxation times* for electrical and mechanical stresses acting on liquid or glassy states of the material. This leads to the definition of a conductivity/viscosity mode *decoupling index*, useful as a figure of merit for the solid electrolyte. In applying the same approach to polymer electrolyte systems a problem is encountered due to the molecular weight dependence of the viscosity. This is resolved by deriving a "monomer" shear relaxation time for the polymer electrolyte solution and showing that this quantity corresponds closely with the "local" mechanical relaxation time obtained from light scattering studies (which is a molecular weight independent quantity for pure polymers). Comparison of the electrical relaxation times of the polymer solution with the "local" (or "matrix") relaxation times then shows that the relationship found for superionic glassforming systems is inverted in the case of polymer electrolytes. The latter have fractional decoupling indexes which may be interpreted in terms of serial coupling phenomena; i.e. ions must first decouple from their partner ions (in ion pairs), or from their intramolecular solvation states, before they can contribute to conductivity relaxation which is itself coupled to the local polymer matrix relaxation. An extreme case is illustrated using the weak electrolyte, lithium acetate, for which the decoupling index is $\sim 6 \times 10^{-5}$.

ION-MATRIX COUPLING IN POLYMER ELECTROLYTES FROM RELAXATION TIME STUDIES

L.M. Torell
Department of Physics
Chalmers University of Technology
Goteborg, S-41296, SWEDEN

and

C.A. Angell
Department of Chemistry
Purdue University
West Lafayette, IN 47906, USA

INTRODUCTION

In this paper we show how the combination of light scattering⁽¹⁾ and conductivity⁽²⁾ data can provide a phenomenological scheme for the discussion of conductivity in relation to polymer chain segmental motion in polymer electrolytes. This scheme permits the relationship between different polymer/salt systems and (the alternative) solid electrolyte systems based on inorganic glasses to be clearly seen. Hopefully, the basis we propose for organizing observations on polymer systems will make it simpler to define the limiting factors on polymer electrolyte performance and lead to improvements in that performance.

It is generally recognized that the mechanism for conductance in polymer-salt systems is intrinsically different from that in fast ion conducting glasses. In the former a highly flexible polymer backbone structure is essential. This has the concomitant requirement that the glass transition phenomenon, which signals the "bottom" of the liquid-like regime of behavior, lies at temperatures far below that of the application. The polymer "solid" electrolyte then owes its mechanical stability to the chain entanglement phenomenon, or to crosslinking in the case of shorter chains. On the other hand, it is obvious that in the case of fast ion conducting glasses (which are no more than deeply supercooled ionic liquids), the glass transition temperature must lie above the temperature of intended application if the electrolyte is to have a fixed shape. Since a "good" performance in each type of system is defined by having d.c. conductivities no less than $10^{-3} \Omega^{-1} \text{ cm}^{-1}$ at the intended service temperature, it is clear that in the superionic glass case the mobile ion motions must be essentially independent of the modes of motion which determine the glass transition. In the polymer electrolyte case, by contrast, the two types of motion must be closely related. Indeed, it is now

the general view that ions in polymer-salt systems move cooperatively in some manner with the segmental motions of the polymer. It is with the definition and interpretation of the time scales for these processes that this contribution is concerned. It will be seen that light scattering techniques applied to polymer solvents⁽³⁻⁶⁾ and recently to polymer solutions⁽¹⁾ provide the most direct relevant probes of the polymer (or "matrix") time scales.

FAST ION CONDUCTING GLASSES

For our investigation of polymer-salt solution behavior, it will be helpful to briefly review the related scheme that has been used to discuss fast ion conduction in liquid and glassy solids⁽⁷⁾. This scheme takes the equilibrium liquid state as its starting point.

In the ionic liquid state, in contrast to polymer electrolytes above T_g , the electrical conductivity is extremely high. For instance, at 150° above its T_g the conductivity of the most simply constituted "superionic" glass, $\text{CsAg}_4(\text{ICl})_5$ is $0.4 \Omega^{-1} \text{cm}^{-1}$ ⁽⁸⁾ (cf $\sim 10^{-3}$ for the best polymer electrolyte⁽⁷⁾). Between $(T_g + 150^\circ)$ and T_g (at -21°C), the conductivity of this material decreases by only some three orders of magnitude. The viscosity, however, increases by more than 15 orders of magnitude in the same T-range. Evidently, unlike the classical Walden electrolytes, the conductivity process is not closely coupled to the viscosity in these systems, except at very high temperatures. This behavior is similar in character to that known for diffusion of gases or small molecule solutes in polymer solutions⁽⁹⁾.

Such differences in the effect of temperature change on transport processes can be presented in a useful manner by comparing the time scales on which the system responds to the stresses which drive the processes. These response times, or *relaxation times* τ , may be obtained directly from frequency-dependent studies of the conductance process (by a.c. admittance bridge techniques)^(9,10) and of the viscous flow process (by ultrasonic absorption⁽¹¹⁾ and Brillouin scattering⁽¹²⁾ techniques) or indirectly by the use of Maxwell relations⁽¹³⁾

$$\langle \tau_\sigma \rangle = e_0 \rho_{dc} / M_\infty \quad (1)$$

and

$$\langle \tau_\eta \rangle = \eta_s / G_\infty \quad (2)$$

which connect liquid-like properties, d.c. resistivity ρ_{dc} , and shear viscosity η_s , to solid-like properties, electrical modulus M_∞ ($M_\infty = 1/\epsilon_\infty$, ϵ the dielectric constant) and shear modulus G_∞ , and ϵ_0 is the permittivity of free space. Eqs. (1) and (2) yield average relaxation times $\langle\tau\rangle$, while the frequency-dependent studies give directly the most probable value and also information on the "distribution of relaxation times" if the relaxation process is non-exponential.

When the data are presented in this manner one observes that at high temperatures the electrical and mechanical response times, τ_σ and τ_s , are rather close, suggesting comparable relaxation mechanisms or a coupling of mechanisms. However, with decreasing temperature (and increasingly well-defined short and intermediate range order of the liquid) the two response times separate increasingly (see Fig. 1 below), implying a progressive *decoupling* of the mechanisms. The ratio of the relaxation times τ_s/τ_σ reflects the decoupling and has been called the *decoupling index*, $R_d^{(7)}$. Its value at the glass transition temperature T_g where the intermediate range order becomes frozen for all lower temperatures, has been suggested as a figure of merit for fast-ion conducting (FIC) glasses.

We will use the same index in this paper as a figure of merit for polymer-salt electrolytes, though the values of maximum merit will be seen to differ by some 14 orders of magnitude from those of high performance FIC glasses. To provide an example with which to compare polymer electrolyte behavior we show in Fig. 1 the relation between viscosity and conductivity relaxation times obtained from ultrasonic⁽¹¹⁾ Brillouin scattering⁽¹²⁾, shear viscosity⁽⁸⁾, and conductivity^(8,10) data for liquid and glassy states of two vitreous systems, using a reduced Arrhenius plot presentation with T_g scaling. One of the systems, AgI-AgCl-CsCl, yields a superionic glass⁽¹⁴⁾, while the other, $2\text{Ca}(\text{NO}_3)_2 \cdot 3\text{KNO}_3$ yields a low-conducting glass^(10b).

POLYMER-SALT SOLUTIONS

(a) Mechanical Responses.

To examine the coupling relations for polymer-salt solutions we must first clarify the relation between viscosity-based and other relaxation times. To this end we examine basic data for a fully amorphous polymer-salt system, PPG + sodium triflate (NaCF_3SO_3) using solvents of molecular weight 425 and 4000. We choose a salt concentration such that the ratio of monomer units $(-(\text{CH}_2\text{CH}_3)-\text{CH}_2-\text{O}-)$ to salt units, Na

CF_3SO_3 , (written $[-\text{O}-]/[\text{Na}^+]$) is 16:1 in each case. This concentration is on the high concentration side of the conductivity maximum for this system if, as expected, it behaves like LiClO_4 in PPG⁽¹⁵⁾. Details on the measurements are to be found in a report of more extended studies being published elsewhere^(1,2).

Fig. 2 shows an Arrhenius plot of rotating spindle viscosity data for the solutions. The data extend over two orders of magnitude. We include viscosity data for the pure solvents taken from the literature^(16,17). Fig. 3 shows the results of a Brillouin scattering study of the 4000 MW solution. Absorption coefficients α/n (n = refractive index) for $\sim 5.3\text{GHz}$ sound waves, obtained in the manner recently described for the pure PPG solvents^(5,6) are plotted as a function of temperature. At the absorption maximum the condition $\omega_B \tau_1 = 1$ is satisfied so, at 107°C , we find that the relaxation time τ_1 for longitudinal stresses is 3×10^{-11} sec. Based on the results for non-polymeric liquids^(12,18), (see Fig. 1), this will also be the relaxation time for shear stress at hyper-sonic frequencies.

To compare this latter value with the relaxation times characterizing the macroscopic viscosities of Fig. 2 we must use the Maxwell relation, Eq. 2. Lacking G_∞ data for the solution at this time, we use the values found for the pure solvents of comparable molecular weight by Lamb and Erginsav using an ultrasonic technique⁽¹⁷⁾. Since the glass transition temperatures differ by only $\sim 20\text{K}$ (see below) and since G_∞ usually scales with T_g , this substitution will not lead to errors in excess of 10%. As will be seen the effects of interest to us are orders of magnitude in τ , so the G_∞ choice is not an important source of uncertainty.

Using the expression

$$G_\infty^{-1} = 1 \times 10^{-10} + 1.85 \times 10^{-11} (T - 180.1) \quad (3)$$

for the 4000 molecular wt. polymer⁽¹⁷⁾, and the viscosity data of Fig. 2, we obtain the average shear relaxation times $\langle \tau_s \rangle$ shown as open circles in Fig. 4. As expected these times are much longer than for the value obtained from Brillouin scattering (open square). The latter is independent of molecular weight for pure PPGs and appears to reflect some local process,⁽³⁻⁶⁾ while viscosities in polymers increase as the first power of the molecular weight up to the chain entanglement point⁽¹⁹⁾.

We now test the proposal⁽³⁻⁶⁾ that the Brillouin relaxation time is a truly microscopic relaxation time by comparing its value with that of a derived local relaxation time $\langle \tau_{s,1} \rangle$ obtained by extrapolating the molecular weight-dependent shear relaxation

time back to the single repeat unit limit. We obtain $\langle \tau_{s,1} \rangle$ from the obvious relation

$$\langle \tau_{s,1} \rangle = \langle \tau_{s,n} \rangle / n \quad (4)$$

where n is the number of repeat units ($-\text{[CH-CH}_3\text{]-CH}_2\text{-O-}$) in the average chain, viz., 69 for the 4000 PPG and 7 (including end oxygens) for 425 PPG. The values of $\langle \tau_{s,1} \rangle$ from the PPG 4000 solution are plotted as filled circles in Fig. 4 where it is seen that they fall very close to (at slightly shorter times than) the Brillouin value. We use a reduced temperature scale in Fig. 4 in order to incorporate $\langle \tau_s \rangle$ values for other Na triflate solutions and τ_1 data for pure PPG. To avoid confusion in Fig. 4, we do not include $\langle \tau_{s,1} \rangle$ values from the 425 MW solutions, but note here that they fall systematically 0.3 log units to shorter times than those from the 4000 MW solution. The difference may well be due to different salt effects on the pure solvent G_∞ values we were obliged to use in the calculation of $\langle \tau_{s,n} \rangle$, hence $\langle \tau_{s,1} \rangle$ values.

To further support the correlation of Brillouin and "monomer" shear relaxation times, we may add data from the literature for the pure PPG solvents. The dashed line in Fig. 4 is the light scattering-based longitudinal relaxation time for pure PPG 4000 and other molecular weights taken from a recent paper⁽⁵⁾ in which short time Brillouin scattering data were combined with the longer time (10^{-1} – 10^{-4} sec) digital correlation spectroscopy results of Wang et al.⁽³⁾ Here it is plotted using $T_g = 201\text{K}$ as scaling parameter. Since both the Brillouin study⁽⁶⁾ and the DCS study⁽³⁾ of PPG's in the MW range 400 - 5,600 find only a very weak molecular weight dependence, and since T_g is likewise independent of MW, the dashed curve in Fig. 4, is also molecular weight-independent, at least for pure solvents. The small displacement of the salt solution $\tau_1(\text{BS})$ point (square) from the the pure solvent value (dashed line) may be partly due to the choice of T_g value 218K used in the temperature scaling (see below) but could also reflect real changes in the temperature dependence of the relaxation time as the salt cations transiently cross-link the polymer chains.

On the basis of the findings in Fig. 6 we conclude that light scattering measurements, or chain number-reduced viscosity measurements, may provide data on local structural relaxation times in polymer electrolytes which are equivalent to the $\langle \tau_s \rangle$ values with which the electrical relaxation time was compared in the case of the liquid and glassy inorganic electrolytes of Fig. 1.

It is of interest to know how large the locally relaxing group of segments detected by the light scattering experiment is. The relative placement of the $\langle \tau_{s,425} \rangle$ ($n=7$),

τ_1 (BS), and $\langle\tau_{s,1}\rangle$ points in Fig. 4 suggests that it is larger than one PPG repeat unit, but perhaps smaller than seven*. It may also depend a little on salt concentration (which should have some influence on the refractive index fluctuations detected by light scattering) since comparison of $\langle\tau_{s,1}\rangle$ values for pure PPG 4000 solvent (not shown in Fig. 4) with light scattering values shows twice the gap between τ_1 (BS) and $\langle\tau_{s,1}\rangle$ seen in Fig. 4 for the solution data.

(b) *Electrical Relaxation Times, and Coupling Relations.*

With a plausible measure of the relevant matrix relaxation time now available, electrical relaxation times are required for comparison. In Fig. 5 we show real M' and imaginary M'' parts of the electrical modulus M^* ($M^* = 1/\epsilon^*$)⁽¹³⁾ obtained from automated admittance bridge measurements on the R=16 sodium triflate solution in PPG 4000 in the temperature range -20 to +22°C. The solution was contained in an all-metal cell to avoid spurious second dielectric effects which may arise when glass containers are used with low conducting solutions. Details are available elsewhere⁽²⁾.

Fig. 5 contains, for comparison, the M'' vs. frequency plot for a system relaxing with a single relaxation time with the same value as the most probable relaxation time for the present triflate solution at -20°C, see dashed curve. The comparison makes clear that the triflate solution, at this concentration at least, is complex and is characterized by a very broad spectrum of relaxation times. This is also indicated by the unusually smeared-out glass transition for this composition shown, along with data for the PPG 425 triflate solution and the pure solvents, in Fig. 6. The origin of the complexity will be dealt with elsewhere⁽²⁾. It is sufficient to note here that the broad loss curves of Fig. 5 cannot be well fitted with the usual Williams-Watts function.

We now take the most probable conductivity relaxation times from the M'' peak frequencies of Fig. 5, $\tau_\sigma = 1/2\pi f_{\sigma, \max}$, and plot them in Fig. 7 together with the "monomer" shear relaxation times, and the Brillouin relaxation time from Fig. 4. The conductivity relaxation time plot may be extended to higher temperatures by including average conductivity relaxation times $\langle\tau_\sigma\rangle$ obtained from the d.c. conductivities and

* It is interesting to note that the $\omega\tau=1$ condition in ultrasonic relaxation of the pure PPG's although also much less dependent on molecular weight than viscosity, occurs at much larger times than in Brillouin scattering and indeed at even larger times than the shear relaxation time for the 4000 MW.⁽¹⁷⁾ The ultrasonic relaxation is also more nearly exponential than in the hypersonic case, and presumably probes a quite different process.

Eq. (1), with M_{∞} taken as the value of M' in Fig. 6 at three decades above the M'' maximum.

Comparison of Fig. 7 and Fig. 1 shows that in polymer electrolytes the coupling relations are the opposite of those found in the FIC glass case: the electrical field is now relaxed more slowly by ionic migration than is local mechanical stress. Quantitatively, the decoupling index R_c , which we suggest as a figure of merit for 16:1 sodium triflate in PPG 4000, is $\sim 2 \times 10^{-2}$, independent of temperature. This implies that the solvent or matrix structural rearrangements, while obviously necessary for charge migration to occur, are not always accompanied by charge migration.

This latter conclusion may be interpreted in different ways. The most obvious one would be in terms of ion pairing phenomena which are anticipated in low dielectric constant media, and which have been observed spectroscopically^(20,21) and quantitatively evaluated in one case.⁽²¹⁾ Conductivity relaxation does not occur if a structural relaxation is accompanied by the displacement of a bound ion pair because no net charge displacement occurs (provided we restrict considerations to solutions of the 1:1 electrolytes which are of principal interest to solid electrolyte studies). The almost constant displacement of the τ_0 plot from the τ_1 (local relaxation) plot is consistent with evidence⁽²¹⁻²³⁾ that the population of ion pairs is only a weak function of temperature.

To show this effect unambiguously we include, in Fig. 7 some conductivity relaxation data⁽²²⁾ from a 40:1 solution of lithium acetate in PPG 425 (higher concentrations not being easily obtained). Lithium acetate is a weak electrolyte in polymer solutions, its conductivity being smaller by \sim three orders of magnitude than for the corresponding LiClO_4 solution.^(15,24) Since the electrical modulus is not greatly changed from the pure solvent value by the presence of the lithium acetate, the τ_0 values reflect the conductivity, and fall at much longer times than the structural relaxation time. The decoupling index in this case is $\sim 6 \times 10^{-5}$. It is appropriate to think of such a value as a reflection of a serial coupling phenomenon viz. in order to migrate via a solvent-coupled mechanism, the ion must first decouple from its ion-paired partner.

The second way in which the reversal of the FIC glass coupling relations may be interpreted is in terms of *intra* vs. *intermolecular* solvation phenomena. The migration of an ion in an electrical field will presumably be freer if it can exchange solvation by one chain oxygen to solvation by oxygens of neighboring chains. Statistically, intramolecular solvation should be less pervasive in solutions with lower molecular

weight chains than in high MW solvent solutions. This may be the reason that τ_g is closer to $\langle\tau_{s,1}\rangle$ in the case of the 425 PPG solution than in the case of the 4000 PPG solution of equal $[-O-]/[Na^+]$, see Fig. 7.

These considerations are in a preliminary stage of development, and clearer correlations and interpretations will be possible when additional experimental data are at hand.

Acknowledgements:

The authors are indebted to the U.S. National Science Foundation, Office of International Programs for support of this collaborative project under Grant No. INT 8619785, and to the Swedish Natural Sciences Research Council and the U.S. Office of Naval Research Agreement No. N00014-84K-0289 for support of the experimental studies on which our analysis has been based. We are grateful to a number of our coworkers, S. Schantz, J. Sandahl, L. Borjesson, M. McLin, Rongjian Xue, and A. Kulkarni for their willingness to let us use some of their unpublished results in support of the ideas presented in this manuscript.

REFERENCES

1. S. Schantz, J. Sandahl, L. Borjesson and L.M. Torell, (to be published).
2. M. McLin and C.A. Angell (to be published).
- 3a. C.H. Wang and Y.Y. Huang, J. Chem. Phys. 1976, 64, 4847.
- 3b. C.H. Wang, G. Fytas, D. Lilge, and Th. Dorfmueller, *Macromolecules*, 14, 1363, (1981).
4. G.D. Patterson, D.C. Douglass, J.P. and Latham, *Macromolecules*, 1978, 11, 263.
5. L. Borjesson, J.R. Stevens, and L.M. Torell, *Polymer*, (1987), in press.
6. L. Borjesson, J.R. Stevens, and L.M. Torell, *Physica Scripta*, 35, 0000, (1987), (in press).
7. C.A. Angell, *Solid State Ionics*, 9 & 10, 3 (1983); 18 & 19, 72 (1986)
8. M. McLin and C.A. Angell (to be published), C.A. Angell, *Materials for Solid State Batteries*, ed. by B.V.R. Chowdari and S. Radhakrishna, p. 31-40 (1986).

9. gases in polymers

- 10a. C.T. Moynihan, R.D. Bressel and C.A. Angell, *J. Chem. Phys.*, **55**, 4414 (1971).
- 10b. F.S. Howell, R.A. Bose, P.B. Macedo and C.T. Moynihan, *J. Phys. Chem.* **78**, 639, (1974).
11. R. Weiler, R. Bose and P.B. Macedo, *J. Chem. Phys.* **53**, 1258 (1970).
12. L.M. Torell, *J. Chem. Phys.* **76**, 3467, (1982).
- 13a. P.B. Macedo, C.T. Moynihan and R.A. Bose, *Phys. Chem. Glasses*, **11**, 171, (1972).
- 13b. J. Wong and C.A. Angell, "Glass Structure by Spectroscopy," M. Dekker, N.Y., 1976, Chapter 11.
14. Changle Liu, H.G.K. Sundar and C.A. Angell, *Mat. Res. Bull.*, **20**, 525 (1985).
15. M. Watanabe, J. Ikeda, and I. Shinohara, *Polymer J.*, **15**, 65, (1983): **15**, 175, (1983).
16. M.E. Baur and W.H. Stockmayer, *J. Chem. Phys.*, **43**, 4319, (1965).
17. A.J. Lamb and A. Erginsav, *Polymer*, **16**, 110, (1975).
18. C.A. Angell and L.M. Torell, *J. Chem. Phys.*, **78**, 937 (1983).
19. G.C. Berry and T.G. Fox, *Adv. Polymer Sci.*, **5**, 261, (1968).
20. D. Teeters and R. Frech, *Solid State Ionics*, **18 & 19**, 271, 1986.
21. S. Schantz, J. Sandahl, L. Borjesson and L.M. Torell, *Solid State Ionics* (1988) (to be published).
22. M.C. Wintersgill, J.T. Fontanella, S.G. Greenbaum and K.J. Adamic *British Polymer J.*, (1987) (in press).
23. M. Watanabe, K. Sanui, N. Ogata, T. Kobayashi and Z. Ohtaki, *J. Appl. Phys.*, **57**, 13, (1985).
24. Rongjian Xue and C.A. Angell (to be published).

FIGURE CAPTIONS

Figure 1.

Average mechanical (shear) and electrical relaxation times, $\langle\tau_p\rangle$ and $\langle\tau_o\rangle$, for liquid and glassy states of the fast ion conductor AgCl/AgI/CsCl and the poor conductor $2\text{Ca}(\text{NO}_3)_2/3\text{KNO}_3$. In the latter case, the shear relaxation times coincide with the longitudinal relaxation time determined by Brillouin scattering $\tau_l(\text{BS})$. Also note the close correspondence between $\langle\tau_p\rangle$ and $\langle\tau_o\rangle$ for $T > T_g$ in this case.

Figure 2.

Viscosity data for PPG solutions of sodium triflate 16:1. Dashed lines are data for pure solvents from Refs. 3b and 16.

Figure 3.

Absorption coefficient α divided by refractive index n as function of temperature for 16:1 sodium triflate in PPG 4000. The peak falls at 107°C , cf 56°C for pure PPG 4000.

Figure 4.

Average shear relaxation times for sodium triflate solutions, 16:1 in PPG 4000, (open circles) and PPG 425 (dotted line) and derived "monomer" relaxation time ($\langle\tau_{s,1}\rangle$) for 4000 salt solution shown in relation to the longitudinal relaxation time of the solution from Brillouin scattering $\tau_l(\text{BS})$ (open square). Longitudinal relaxation times from light scattering for the *pure* PPG solvent of various molecular weights are shown as dashed line.

Figure 5.

Real M' and imaginary M'' parts of the electrical modulus as function of frequency for sodium triflate solution (16:1) in PPG 4000. Dashed line under -20°C curve shows shape of loss spectrum for exponential relaxation (single relaxation time).

Figure 6.

DSC scans of the glass transition phenomenon in pure PPG solvents of MW 425, 4000, and $\sim 10^6$ compared with those for 16:1 solutions of sodium triflate in PPG 425 and PPG 4000. In the latter case the definition of the glass transition is ambiguous.

Figure 7.

Comparison of conductivity relaxation times τ_σ with average shear relaxation times $\langle\tau_s\rangle$ and local structure relaxation times derived from light scattering $\tau_l(\text{BS})$ and "monomer" shear relaxation time $\langle\tau_{s,1}\rangle$, for sodium triflate solutions (16:1) in PPG 4000. Dashed line is light scattering-based longitudinal relaxation time for pure PPG from Ref 5. Also shown are conductivity relaxation times for the weak electrolyte lithium acetate 40:1 in PPG 425 ($T_g = 198\text{K}$). For comparison, the dotted line shows τ_σ of sodium triflate 16:1 in PPG 425.

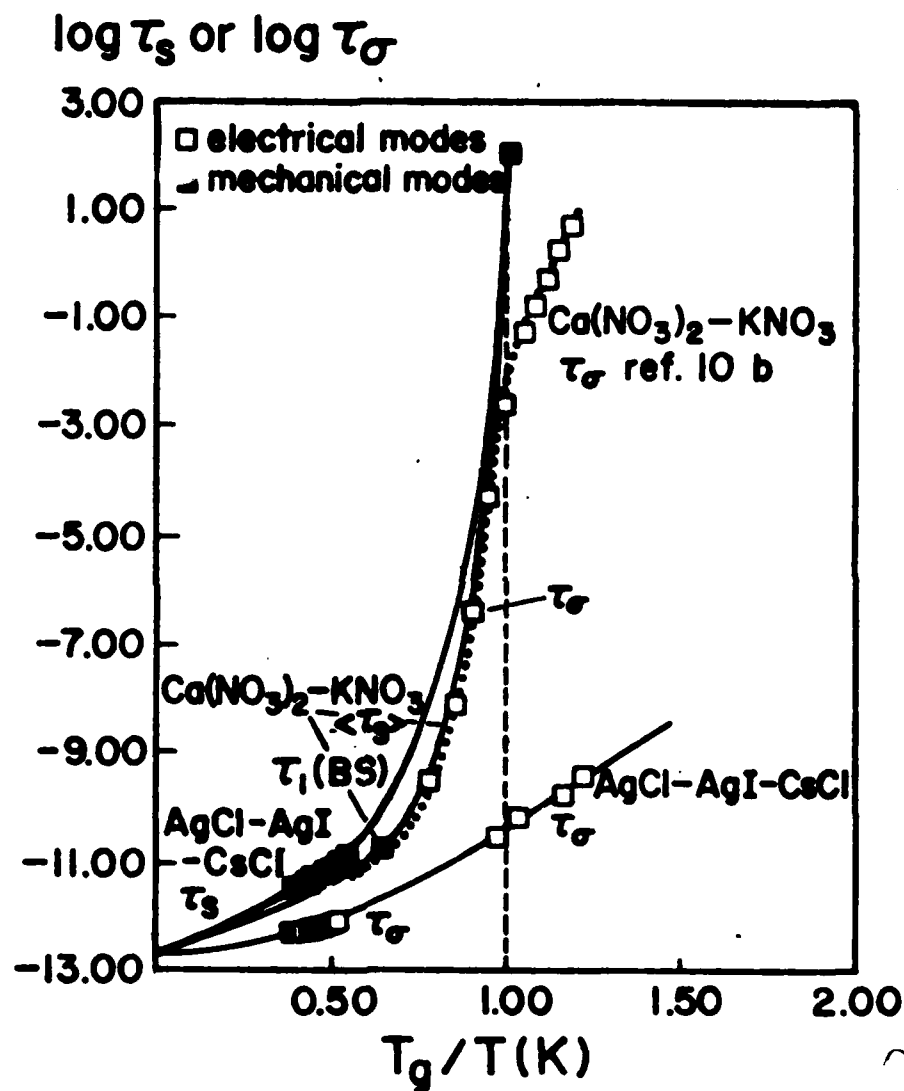


Figure 1.

Average mechanical (shear) and electrical relaxation times, $\langle \tau_s \rangle$ and $\langle \tau_\sigma \rangle$, for liquid and glassy states of the fast ion conductor AgCl/AgI/CsCl and the poor conductor $2\text{Ca}(\text{NO}_3)_2/3\text{KNO}_3$. In the latter case, the shear relaxation times coincide with the longitudinal relaxation time determined by Brillouin scattering $\tau_1(\text{BS})$. Also note the close correspondence between $\langle \tau_s \rangle$ and $\langle \tau_\sigma \rangle$ for $T > T_g$ in this case.

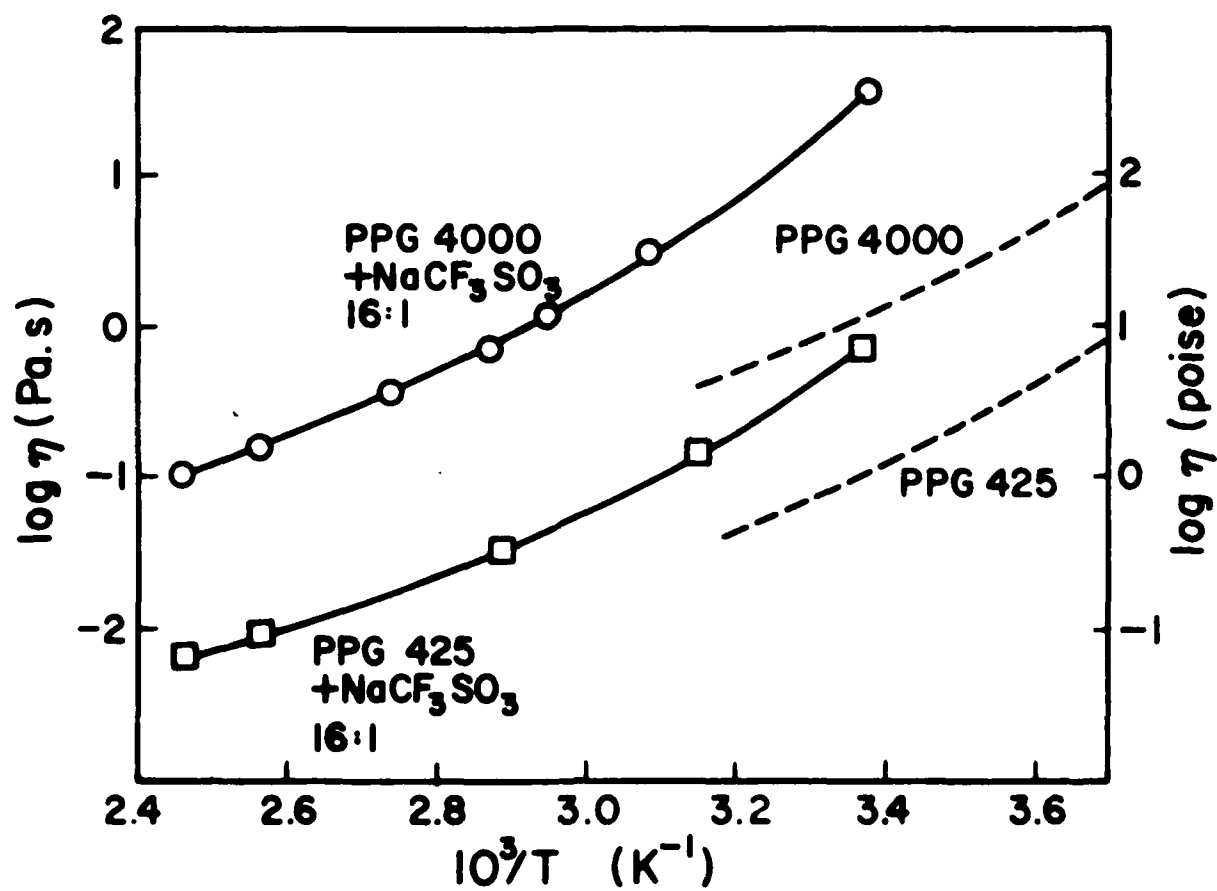


Figure 2.

Viscosity data for PPG solutions of sodium triflate 16:1. Dashed lines are data for pure solvents from Refs. 3b and 16.

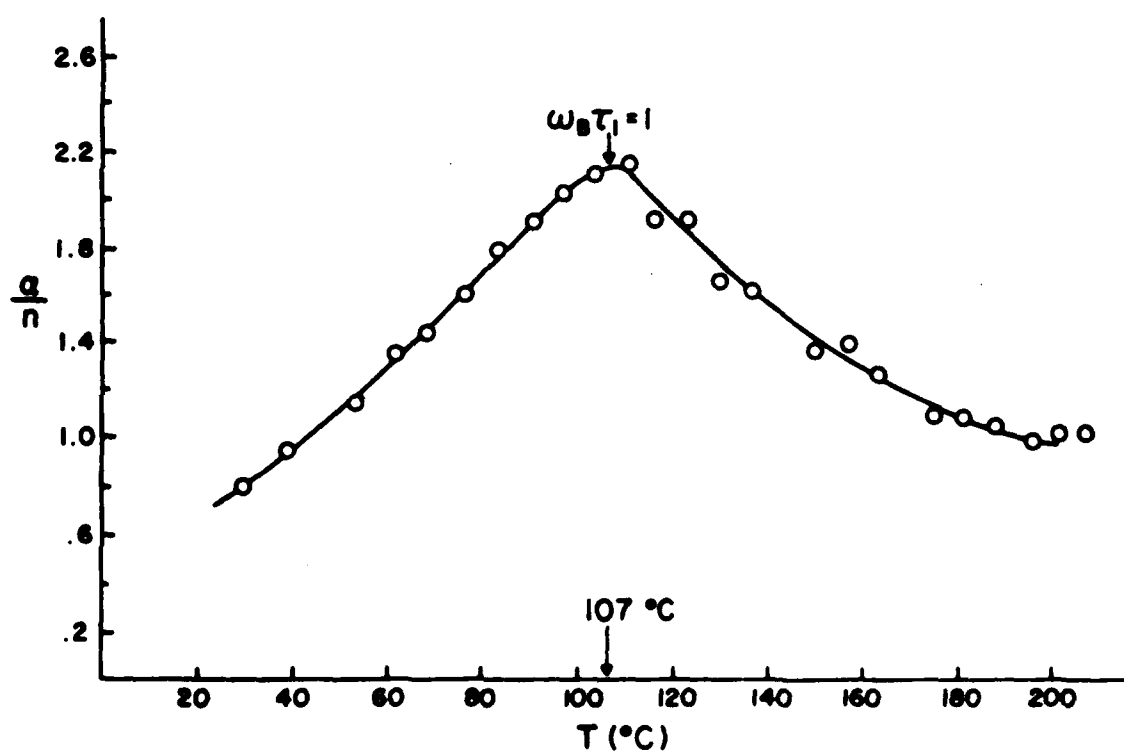


Figure 3.

Absorption coefficient α divided by refractive index n as function of temperature for 16:1 sodium triflate in PPG 4000. The peak falls at 107°C , cf 56°C for pure PPG 4000.

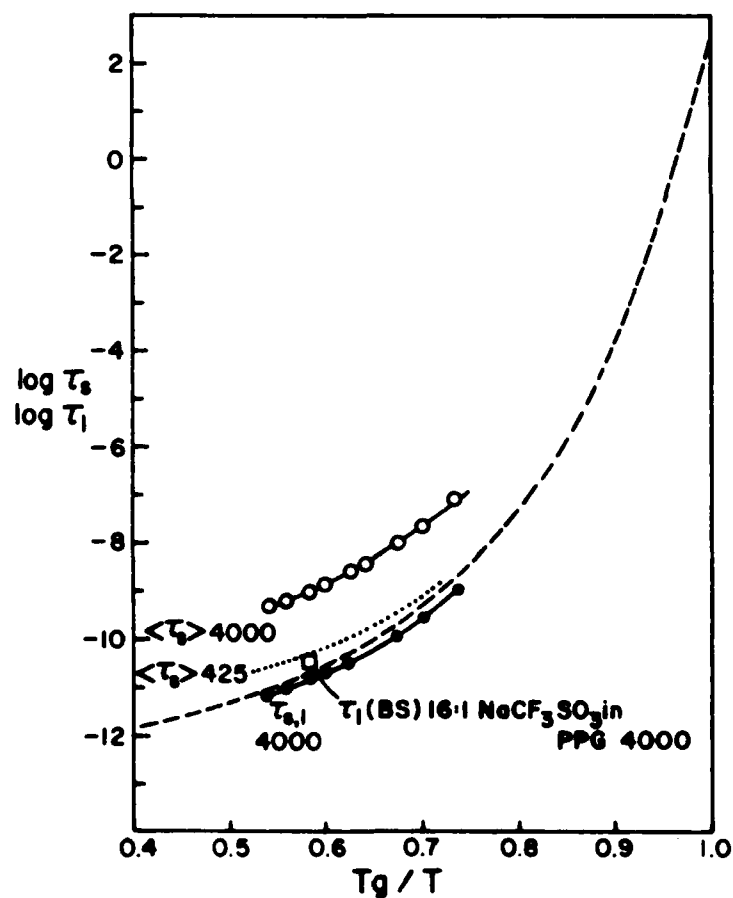


Figure 4.

Average shear relaxation times for sodium triflate solutions, 16:1 in PPG 4000, (open circles) and PPG 425 (dotted line) and derived "monomer" relaxation time ($\langle \tau_{s,l} \rangle$) for 4000 salt solution shown in relation to the longitudinal relaxation time of the solution from Brillouin scattering τ_l (BS) (open square). Longitudinal relaxation times from light scattering for the *pure* PPG solvent of various molecular weights are shown as dashed line.

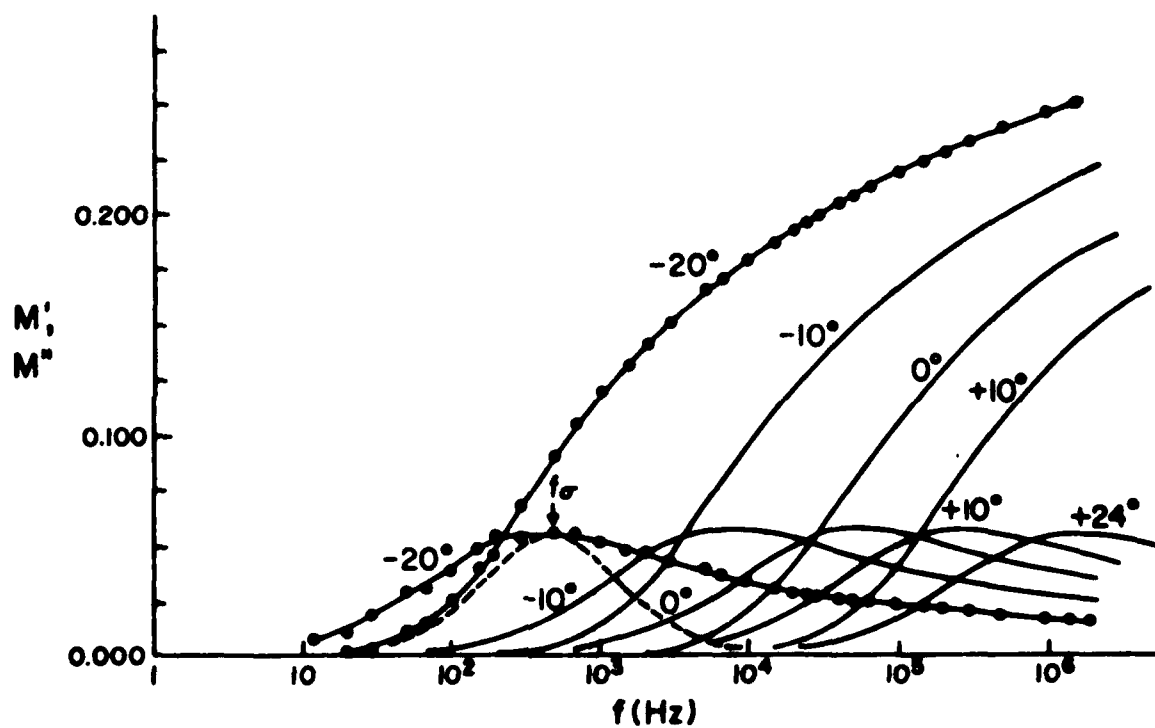


Figure 5.

Real M' and imaginary M'' parts of the electrical modulus as function of frequency for sodium triflate solution (16:1) in PPG 4000. Dashed line under -20°C curve shows shape of loss spectrum for exponential relaxation (single relaxation time).

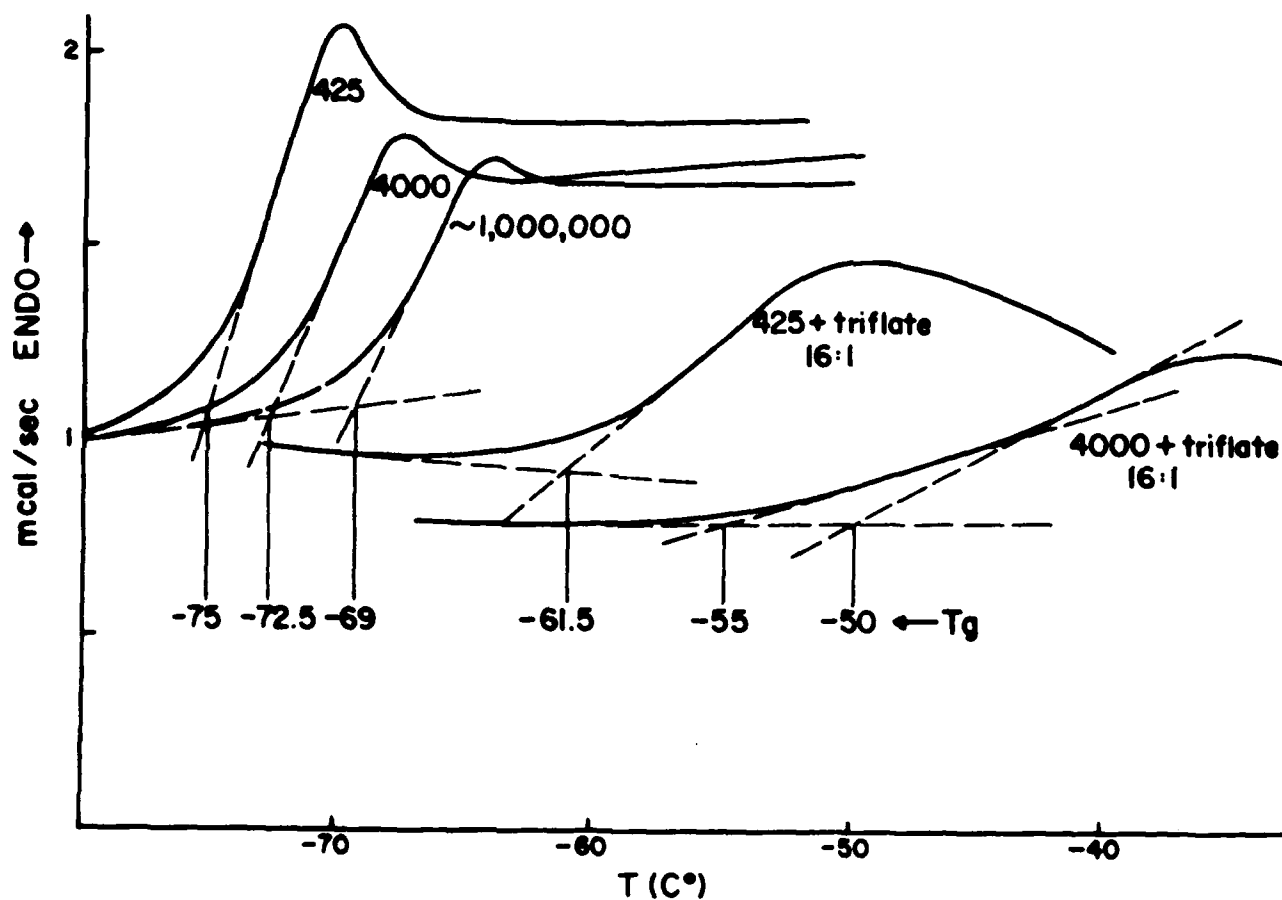


Figure 6.

DSC scans of the glass transition phenomenon in pure PPG solvents of MW 425, 4000, and $\sim 10^6$ compared with those for 16:1 solutions of sodium triflate in PPG 425 and PPG 4000. In the latter case the definition of the glass transition is ambiguous.

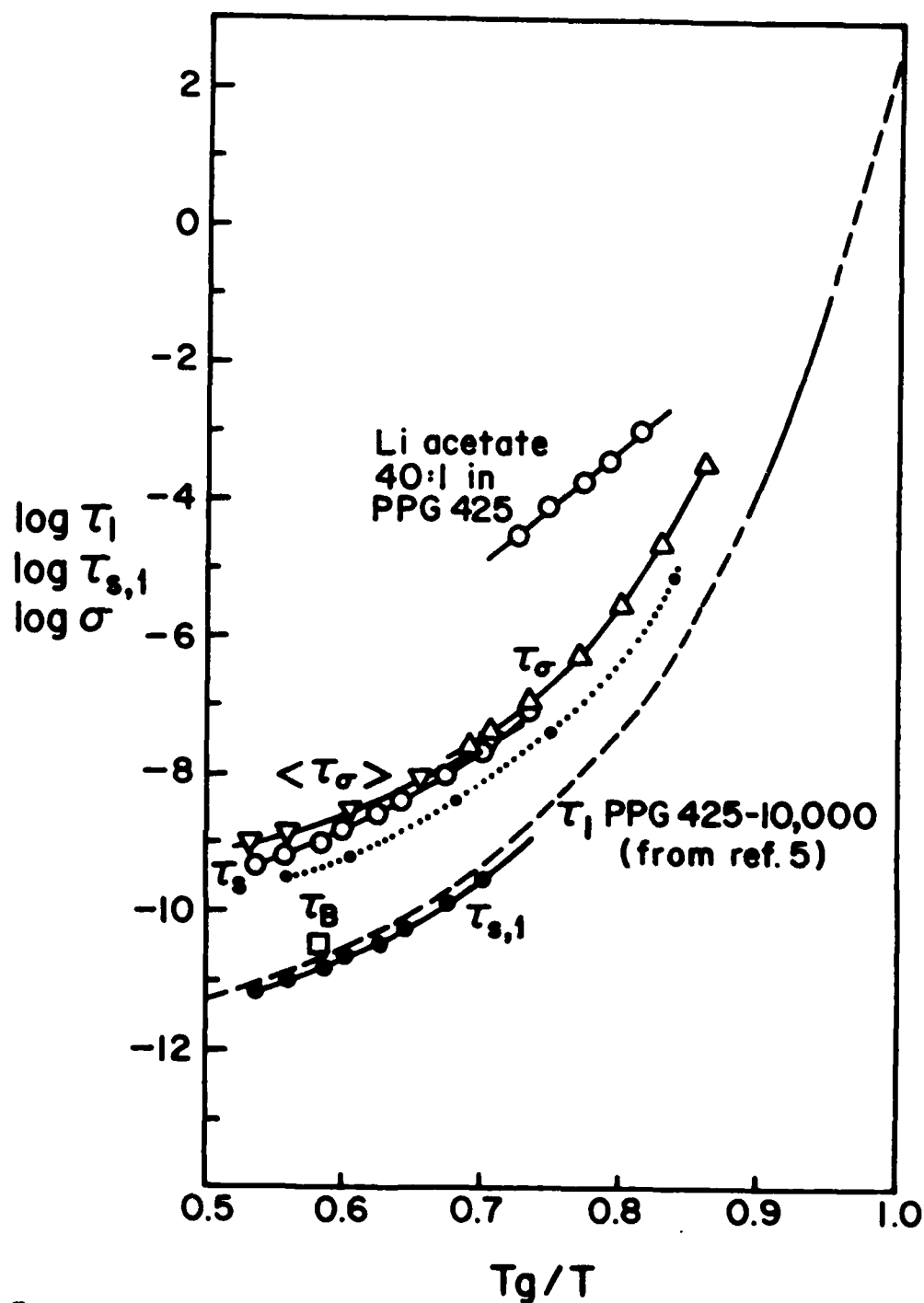


Figure 7.

Comparison of conductivity relaxation times τ_σ with average shear relaxation times $\langle\tau_s\rangle$ and local structure relaxation times derived from light scattering τ_l (BS) and "monomer" shear relaxation time $\langle\tau_{s,1}\rangle$, for sodium triflate solutions (16:1) in PPG 4000. Dashed line is light scattering-based longitudinal relaxation time for pure PPG from Ref 5. Also shown are conductivity relaxation times for the weak electrolyte lithium acetate 40:1 in PPG 425 ($T_g = 198\text{K}$). For comparison, the dotted line shows τ_σ of sodium triflate 16:1 in PPG 425.

END

10-87

DTIC